工學碩士學位論文

Fabrication of palladium nanoparticle decorated silica nanotubes for olefination of aryl iodides

요오드화 아릴의 올레핀화 반응을 위한

팔라디움 나노입자가 부착된 실리카 나노튜브의 제조

2015年 8月

서울大學校 大學院

化學生物工學部

徐 榮 德

Abstract

Fabrication of palladium nanoparticle decorated silica nanotubes for olefination of aryl iodides

Young Deok Seo

School of Chemical and Biological Engineering

The Graduate School

Seoul National University

Preparation of anisotropic material with various functionality has been widely studied and the applications of these fascinating materials in micro/nano size have advantages distinguished from traditional bulk materials. The anisotropic nano material having different in-and-out functional groups can be utilized as selective nanocarrier and smart nanocatalyst. In this paper, silica nanotube was fabricated by vapor phase synthesis (VPS) method using anodic aluminum oxide (AAO) as hard

template for olefination of aryl iodide and carboxylic group was introduced inside the silica nanotube by vapor deposition polymerization (VDP) method. Then, silica nanotube with in-and-out bifunctionality was successfully fabricated by additional hydrophobic silane treatment. Furthermore, palladium nanoparticle can be introduced to silica nanotube with different in-and-out bifunctional group selectively. Then, palladium ion was inserted inside of the nanotube and the palladium ion was reduced by hydrogen gas. The palladium ion can be coordinated with the carboxyl group of bifunctional silica nanotube. Heck reaction for 3 types of olefination of aryl iodides was conducted by Pd-inserted bifunctional silica nanotube and the highest olefination efficiency of 99% was obtained. Our novel approach may open up a new method for fabrication of an anisotropic carrier for nano-catalytic application.

Keyword: silica nanotube, nanocarrier, nanocatalyst, Heck reaction, anisotropic material, Anodic aluminum oxide (AAO)

Student number: 2013-23164

List of Abbreviation

HCl: Hydrochloric acid

VTMS: Vinyl trimethoxy silane

DMA: N,N-Dimethyl acrylamide

TBA: Tributyl amine

CEST: Carboxyethylsilanetriol

APTES: 3-Aminopropyltriethoxysilane

VPS: Vapor phase synthesis

VDP: Vapor deposition polymerization

SEM: Scanning electron microscope

TEM: Transmission electron microscope

AAO: Anodic aluminum oxide

KPS: Potassium persulfate

TTS: Tridecafluoro-1,1,2,2-tetrahydrooctyl triethoxysilane

PAA: Poly (acrylic acid)

EDX: Energy dispersive X-ray spectroscopy

FT-IR: Fourier transform infrared spectroscopy

TGA: Thermogravimetric analysis

TEOS: Tetraethyl orthosilicate

List of Figures

List of Tables

Contents

Chapter 1. Introduction

1.1 Size effect of the nanocatalyst

Until now, tremendous researches have been conducted on nanomaterials and various efforts have been devoted to synthesis of versatile nanomaterials.[1] The reason why nano-sized materials are utilized in various fields is the high surface area and enhanced catalytic properties of nanomaterials.[2] As the particle size decrease, the number of atom on the surface exponentially increase. In Figure 1, a graph shows size effect of the nanomaterial and it describes inversed relation between size and bulk properties.[3]

The increased atoms on the surface act as reactive sites of the reaction between molecules. Herein, as the particles size decreased, the overall properties of the materials are dramatically changed. These phenomena are relevant to quantum confinement effect and nano-sized filler effect as well as finite size effect.[4-6]

The nanocatalysis is the important emerging application of nanomaterials because of high activity, selectivity and productivity of nanomaterials due to high surface area to volume ratio.[7-8] Because of intrinsic characteristics of nanomaterials, the catalysis is the best application for nanomaterials. In particular, nanotube-supported catalysts have been selected for highly efficient catalysis because of their different contact areas that can be functionalized in various ways.[7] Herein, we tried to utilize the anisotropic silica nanotube with palladium nanoparticle for nanocatalyst and the nanotube was applied in olefination of aryl iodides.

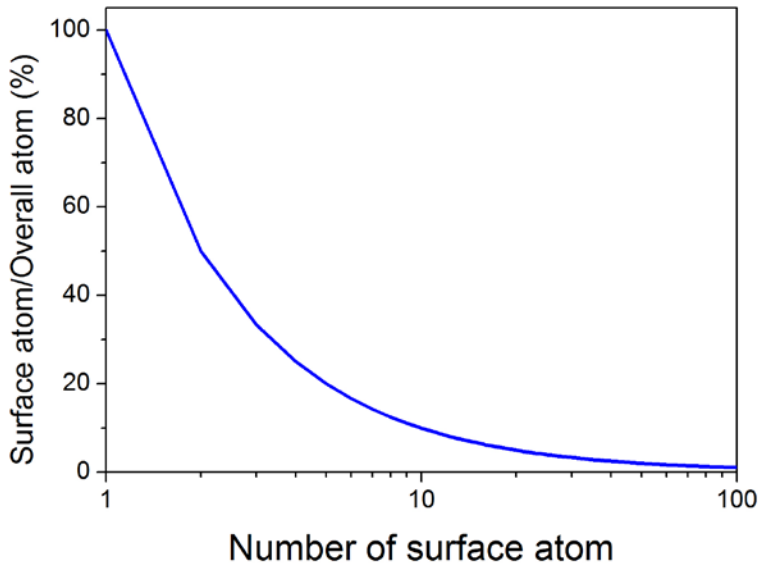

Figure 1. Inverse relationship between the number of surface atom and ratio of surface atom to overall atom.[3]

1.2 Anisotropic building block

Recent efforts on preparation of anisotropic building-block can realize expanding potential application field of nanomaterials.[12-18] Various methods has been conducted to prepare anisotropic building-block and J. Solomon *et al* classified tremendous types of anisotropic particle by dimensional views. [19]

Most of preparation way of anisotropic blocks is based on modification of well-known conventional or bulk particle preparation methods, for example modified microfluidic based methods [20-22], stop-flowing lithography [23-25], and electrospraying methods [26-27].

Among the various anisotropic materials, one-dimensional anisotropic materials with bifunctionality have gained tremendous attention.[28-29] In a manner of vapor phase synthesis and vapor deposition process, one-dimensional anisotropic material with different inner and outer functional group can be easily fabricated. One-dimensional anisotropic nanomaterial with bifunctional group can selectively coordinate metal with inner functional group, which differs from outer surface functional group, and introduction of specific metallic catalyst is possible by choosing appropriate functional group. For this reason, silica nanotube functionalized by silane and functional polymer can be used as nanocatalyst for olefination of aryl iodides.

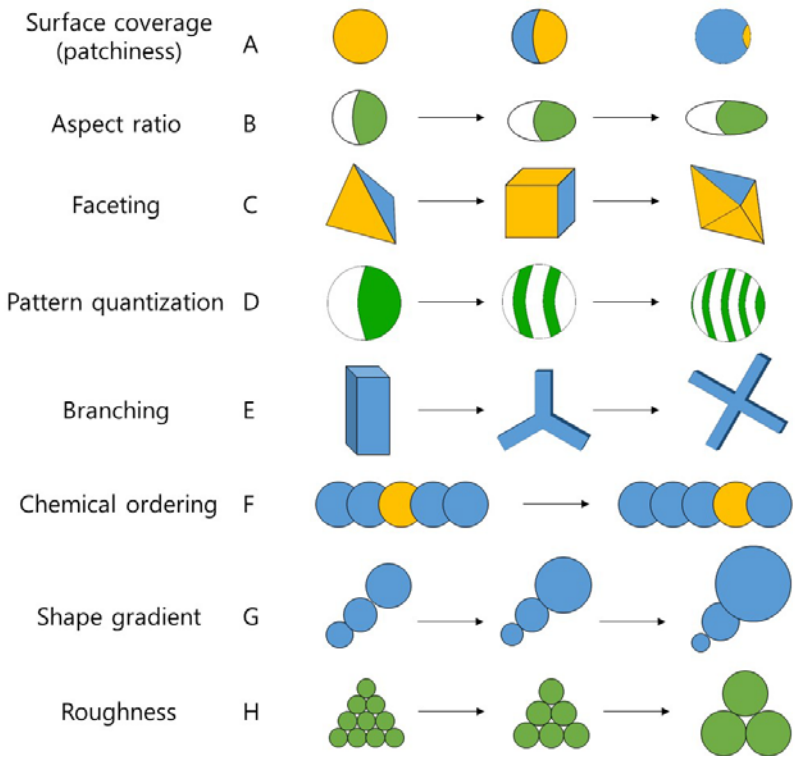

Figure 2. Anisotropy ‘dimensions’ used to describe key anisotropy attributes of particles. Homologous series of particles as the attribute corresponding to the anisotropy axis is varied from left to right.[19]

1.3 Hard template method

Various methods have been utilized for the preparation of one-dimensional nanostructures [30] such as nanotubes, nanorods, polymer nanofibers [31-33] or inorganic materials [34-36]. In particular, hard template methods for fabricating nanomaterials have been widely reviewed in recent years.[37-41]

The widely used kinds of hard template are AAO membrane and track-etched polycarbonate membrane, whose pore size ranges from 10 nm to 100 μm with uniformity. The membrane can be acquired from commercial market and be synthesized easily with regular size in the laboratory using electrochemical method. Because of this simplicity, researchers have used the membranes to synthesize various polymer one-dimensional nanomaterials.[42–47] Especially, using the combined method of utilizing hard template and vapor deposition polymerization (VDP), in a simple manner with a variety of materials, it is possible to make defect-free one-dimensional nanomaterials, without using any special solvent.[31] For example, few years ago, Jang *et al.* produced carbon nanotube (CNT) from carbonization of PPy nanotube prepared by VDP method (Figure 3). [48] And also, the same group fabricated mesoporous silica nanofiber by vapor phase synthesis using AAO as hard template and tetraethyl orthosilicate (TEOS) as silica precursor.[49]

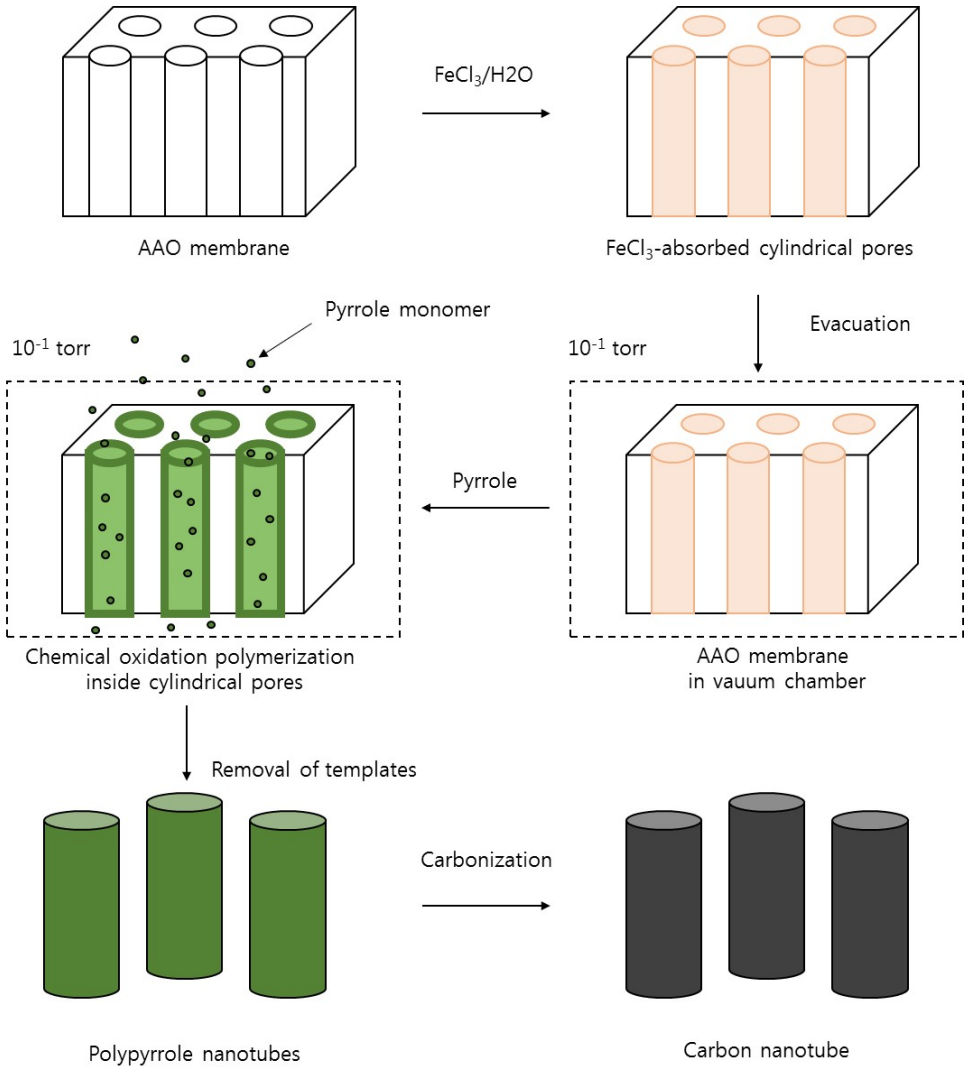

Figure 3. Preparation of carbon nanotube from carbonization of polypyrrole nanotube. Polypyrrole nanotube was synthesized via VDP polymerization of polypyrrole in AAO [31]

1.4 Heck reaction

Approximately 30 years ago, Mizoroki [50] and Heck [51] independently discovered the palladium-based arylation and vinylation of olefins. This methodology, known everywhere as the Heck reaction, has been used among the researchers worldwide, and overall general mechanism is shown in Figure 4.[52-53]

The catalytic cycle of palladium catalyst involves 4 steps: Oxidative addition, coordination insertion, β-hydride elimination-dissociation, reductive elimination and recycling of the Pd(0)[54]. In oxidative addition, except for the case of aryl iodide, the ligands are necessary for effective oxidative addition of RX to the palladium (0) complex at sound temperature.[55-56] In this step palladium elements are inserted in between R-X.

In coordination-insertion, palladium forms a π complex with alkene and alkene inserts itself in the palladium with central point geometry. The insertion process needs a coplanar assembly of metal, ethylene, and the hydride. So, the insertion process is ruled by stereochemistry.

In β-hydride elimination-dissociation, palladium-alkene complex is transformed to a new complex and this complex collapses to produce target product of corresponding reaction. Last, in reductive elimination, palladium (0) compound is regenerated by reductive elimination step with base.

Like styrene and n-butyl acrylate, vinyl-type olefin monomers are useful and versatile precursors for industrial copolymer. However, these monomers usually

polymerize themselves when stored without inhibitors. Thus, Heck reaction of vinyl olefin monomers with aryl iodide might be a practical and useful way. [57]

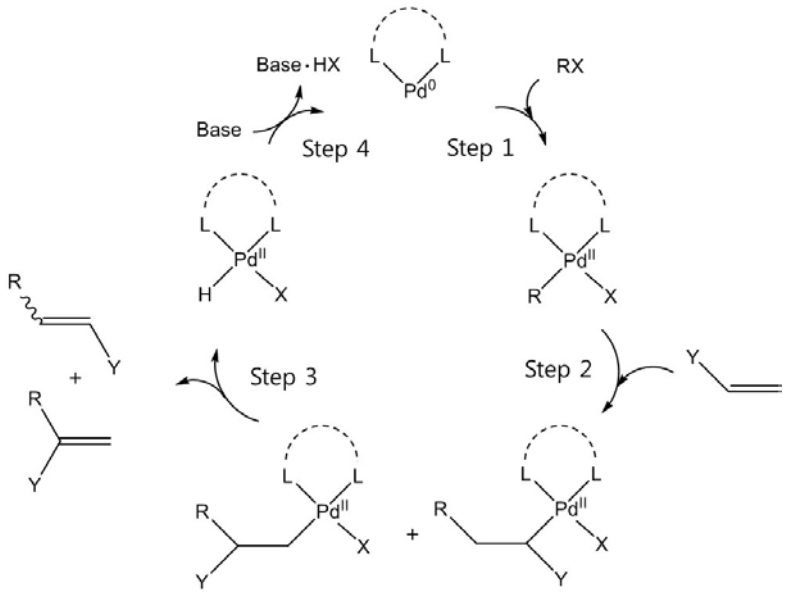

Figure 4. General mechanism of Heck reaction. Step 1) Oxidative addition, Step 2) Cooordination-insertion, Step 3) β-Hydride elimination-dissociation, Step 4) Reductive elimination and recycling of the Pd(0) [52]

1.5 Objective of this study

We present a simple method to prepare silica nanotube via vapor phase synthesis (VPS) method and using AAO membrane as hard template. Several studies to functionalize inner wall of nanotubes using AAO membrane for nanocarrier containing catalyst were conducted, but we prepared further functionalized nanotube with different in-and-out functional group and finally obtained anisotropic silica nanotube. Due to inner carboxyl groups of bifunctional silica nanotube, palladium nanoparticles can easily be coordinated inside the nanotube. And the palladium-inserted bifunctional silica nanotubes are utilized as nanocatalyst for olefination of aryl iodides, showing high catalytic performance. Our approach may open up a new method for the preparation of anisotropic nanotube and might be further utilized in the fabrication of versatile carrier for nanocatalyst.

Chapter 2. Experimental Details

2.1 Materials

Circular anodic aluminum oxide (AAO) film with 25 mm diameter and pore size of 0.2 micrometer was obtained from Whatman, UK. Absolute ethanol (HPLC grade) was purchased from Fisher Scientific, UK. Acrylic acid was supplied from Junsei Chemical Co., Japan. Hydrochloric acid (HCl, 35.0 %~37.0 %), anhydrous toluene, potassium persulfate (KPS, 98 %) and anthracene (99%) were purchased from Samchun Chemical. Co., Korea. Tetraethyl orthosilicate (TEOS, Reagent grade), vinyltrimethoxysilane (VTMS, 98 %), palladium chloride ($PdCl_2$, 99 %), N,N-dimethylacetamide (DMA), tributyl amine (TBA, 98.5%, Reagent grade), iodobenzene (98%), 2-iodotoluene(98%), 3-Aminopropyltriethoxysilane (APTES, 99%), 4-iodoacetophenone(98%), styrene (≥99%, inhibited by 4-tert butyl catechol) and pyrene (99%) were purchased from Sigma-Aldrich Co., USA with no further purification. n-butyl acrylate (98%, inhibited by monomethyl ether hydroquinone) was acquired from Kishida tech, Japan. Carboxyethylsilanetriol (CEST) and Tridecafluoro-1,1,2,2-tetrahydrooctyl triethoxysilane (TTS) were purchased from Gelest. Inc., USA.

2.2 Preparation of silica nanotube

Mixture of distilled water (9 g), absolute ethanol (1.15 g), and hydrochloric acid (0.3 g) was prepared as an initiator solution. AAO film was dipped in the initiator solution for 15 min for complete wetting of inside wall of the AAO pore. After removal of excessive solution on the surface, the AAO membrane was put in the reaction vessel. Then 0.1 ml of TEOS, silica precursor, was put into the reaction vessel separately and the reaction vessel was stored in 80 ^{o}C dry oven for 3 h to initiate vapor phase synthesis. After reaction, the AAO piece was carefully taken from the vessel and was treated with 3M HCl aqueous solution and the solution was put in 100 ^{o}C dry oven for complete etching of AAO substrate. The silica nanotubes were obtained after washing with ethanol for 3 times.

2.3 Preparation of inner-wall-silane-treated silica nanotube

After vapor phase synthesis of silica nanotube inside the AAO wall, the AAO piece was carefully withdrawn from the vessel and washed with distilled water and ethanol for several times. After complete drying, the AAO membrane containing silica nanotube was put into another reaction vessel, and additional VPS was carried out by introducing 0.1 ml of silane liquid (CEST, APTES). After 6 h treatment in 100 ^{o}C dry oven, the AAO membrane was collected from the device and was put into 3M HCl

solution for complete etching of AAO substrate.

2.4 Preparation of inner-wall-PAA-silica nanotube (PAA-silica)

After vapor phase synthesis of silica nanotube inside the AAO wall, the AAO piece was carefully withdrawn from the vial and was washed with distilled water and ethanol for several time. After complete drying, the AAO piece with bundles of silica hollow nanotube was put into 30 ml of 5 % VTMS/toluene solution in round flask. After 12 h treatment in 80 ^{o}C reflux system, the AAO piece was collected from the flask and was washed with toluene several times. After washing process, the vinyl group-treated AAO piece was put into the reaction vessel and the vessel was evacuated for 30 min. Then 0.1 ml of acrylic acid monomer was separately injected into the system and put into 120 ^{o}C dry oven for 15 min for complete introduction of acrylic acid inside the silica nanotube. Then, initiator solution (KPS 0.05 g in 1 ml of water) was injected to completely soak the AAO piece. Then the device was put into 80 ^{o}C dry oven. After 12 h treatment, the AAO piece was put into 3M HCl solution for complete etching of AAO substrate. The PAA-polymerized silica nanotube, PAA-silica, was collected and dried in powder form.

2.5 Preparation of bifunctional silica nanotube (F-PAA-silica)

After complete etching of AAO after polymerization of PAA in silica nanotube, the white powder of PAA-silica were collected. After introducing the powder into the reaction vessel, additional VPS was performed for 6 h at 140 ^{o}C by adding 0.1 ml of tridecafluoro-1,1,2,2-tetrahydrooctyl triethoxysilane (TTS). The as-prepared F-PAA-silica was collected and dried in powder form.

2.6 Preparation of palladium inserted bifunctional silica nanotube (Pd-F-PAA-silica)

After the white powder of F-PAA-silica nanotube was collected, 5ml of nanotube solution (0.5 mg ml^{-1}) was added to 30 ml of $PdCl_2$ solution with different concentration ranged from 1×10^{-4} M ~ 5×10^{-3} M and vigorously stirred for 2 h under nitrogen atmosphere at room temperature. Then, Pd salt were conjugated with carboxylates inside the silica nanotube. After that, palladium ion was reduced by bubbling hydrogen gas into the solution for 2 min. During the reduction, the colour of solution was changed and residual $PdCl_2$ was precipitated. Then, residual $PdCl_2$ was washed by distilled water and product was dried in a vacuum oven at room temperature.

2.7 Heck reaction condition using Pd-F-PAA-silica

All Heck coupling reactions were done at 130 ^{o}C by bifunctional silica nanotube with palladium inserted. The heating mantle was preheated to 130 ^{o}C for reducing temperature gradient during heating the reaction vessel. The reaction was conducted with 20ml of DMA, 3.0 mmol of tributylamine and 2.6 mmol of olefin, 2mmol of pyrene, anthracene in presence of 0.01g of Pd-F-PAA-silica nanotube in nitrogen atmosphere. At the end of the reaction, the reaction vessel was cooled down at room temperature. The yield of the reaction was obtained by quantitative analysis for amount of disappearing reagent peak of gas chromatography/mass spectrometry (GC/MS) comparing that of unreacted substance (pyrene, anthracene).

2.8 Characterization

Scanning electron microscope (SEM) images were obtained with a JSM-6701F (JEOL, Japan). EDX measurement was taken with an INCA energy dispersive X-ray spectrophotometer (Oxford Instruments Analytical Ltd. UK) linked with JSM-6701F SEM. Transmission electron microscope (TEM) images were acquired with a JEM-2100 (JEOL, Japan). Fourier-Transform Infrared (FT-IR) spectra measurement was conducted with a Perkin-Elmer Frontier FT-NIR/MIR Spectrometer, utilizing universal-ATR mode (US). Thermogravimetric analysis (TGA) spectra were also

obtained with a Perkin-Elmer Pyris TGA 6 thermogravimetric analyzer (US). All TGA analyses were conducted in inert nitrogen atmosphere. Zeta potential measurement was taken with an ELS-8000 electrophoretic light scattering spectrophotometer (Otsuka electronics, Japan). All samples for zeta potential measurement were in powder form, which were then dispersed in aqueous solution with pH control. Gas chromatography-mass spectroscopy results were obtained with GMI HP-6890 (GC) and HP-5973 (MS).

Chapter 3. Results and Discussion

3.1 Fabrication of bifunctional silica nanotube (F-PAA-silica)

Figure 5 demonstrates the whole procedure for the fabrication of bifunctional silica nanotube by hard template method and vapor phase synthesis. First, the pristine aluminum oxide (AAO) membrane was cut into two pieces and each piece was dipped in initiator solution. The initiator solution is a mixture of distilled water, absolute ethanol, and hydrochloric acid. After soaking of AAO in the initiator solution for 15 min, the AAO piece was picked up carefully and transferred into reaction vessel. Then tetraethyl orthosilicate (TEOS), silica precursor, was dropped into the vessel separately and the vessel was put into 80 ^{o}C oven for 3 h.[58-59] After vapor phase synthesis of silica nanotube inside the AAO pore, VTMS was initially introduced by thermal treatment method for introduction of vinyl group prior to polymerization of poly (acrylic acid) (PAA). PAA was polymerized by vapour deposition polymerization (VDP), using potassium persulfate as an initiator. The vinyl group of VTMS located in inner layer of silica nanotube act as an initial site for polymerization of acrylic acid.[60-61] After inner functionalization of silica nanotube, AAO template was removed by 3M HCl solution. Then, after harvesting the product, The PAA-polymerized silica nanotube was further functionalized by TTS treatment on the outside the silica nanotube.

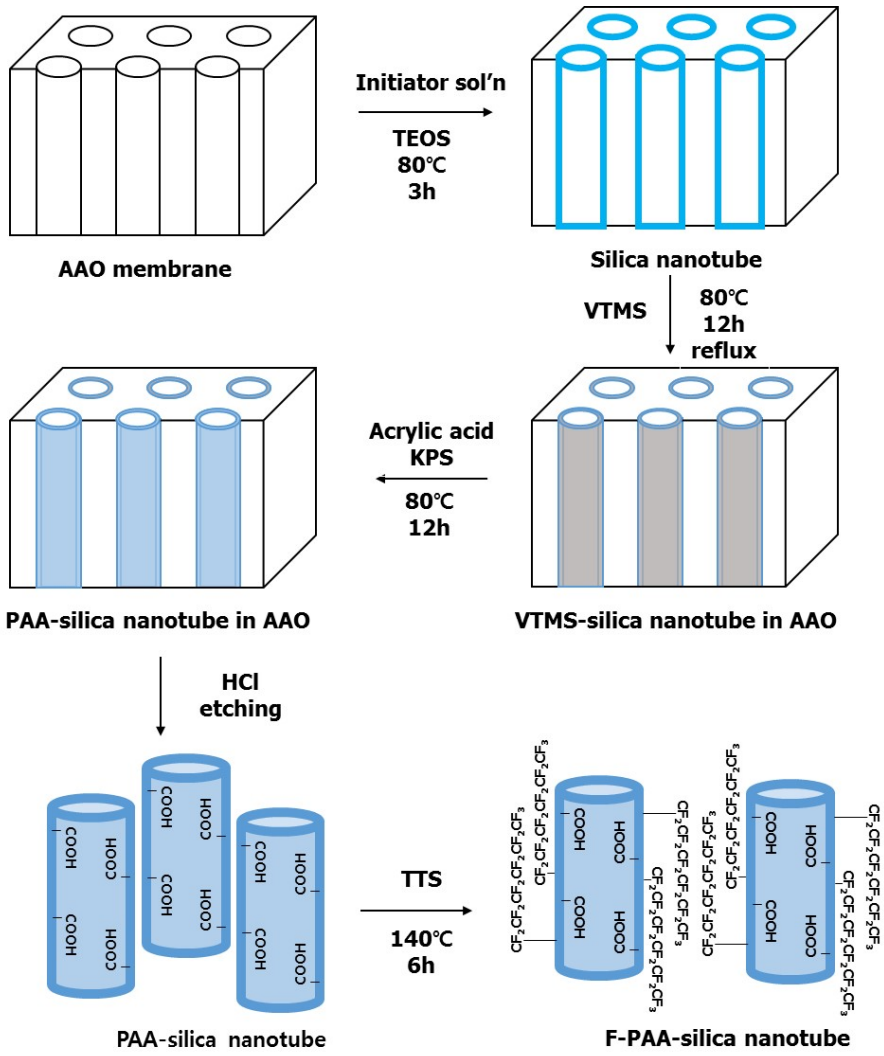

Figure 5. Schematic presentation of overall process.

3.2 Characterization of bifunctional silica nanotube (F-PAA-silica)

3.2.1 SEM and TEM images of pristine silica nanotube

Figure 6a and b shows the scanning electronic microscope (SEM) images of pristine silica nanotubes, illustrating one-dimensional nanostructures with diameter ranging from 200 nm to 300 nm. The variance of diameter is due to the intrinsic pore size variation in the commercialized AAO. Inner hollow structure of nanotubes can be identified by transmission electronic microscope (TEM) images (Figure 7a, and b). The hollow structure was also clarified by holes in the wall of silica nanotube in the SEM image (Figure 6b). In addition, open-pore structure of silica nanotubes can be observed as well (Figure 7b), implying successful preparation of excellent platform for further functionalization of inside wall of nanotubes.

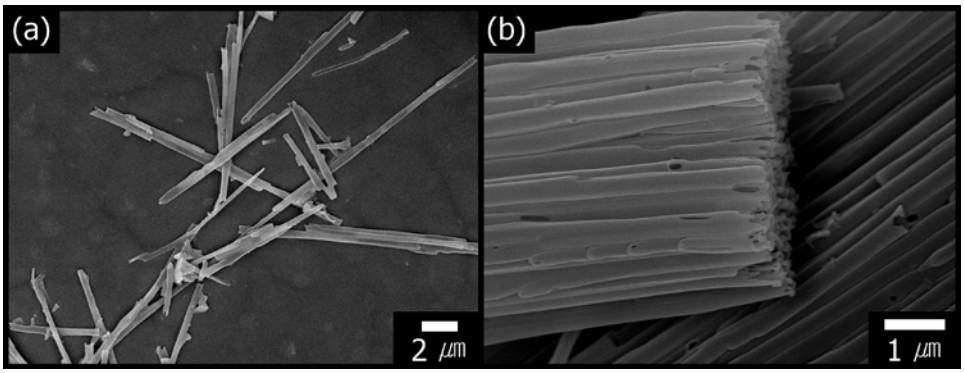

Figure 6. Scanning electron microscope (SEM) images of silica nanotube; (a) Magnification: ×4500, (b) Magnification: ×15000

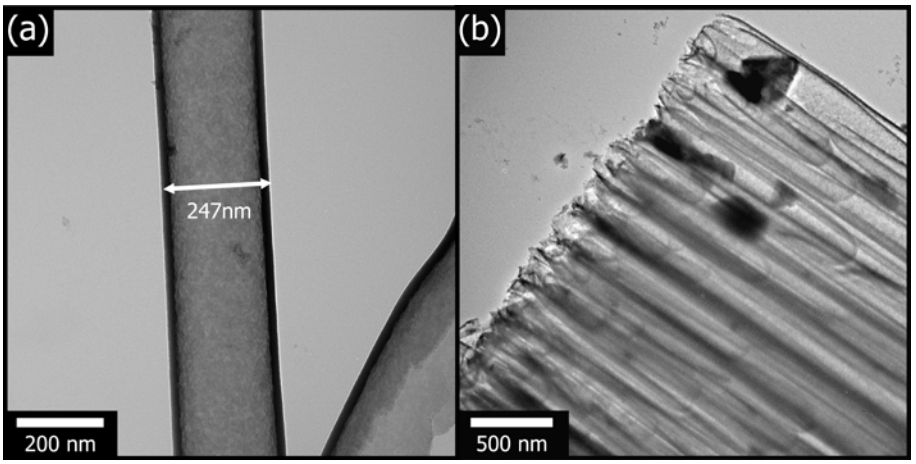

Figure 7. TEM images of pristine silica nanotube by vapor phase synthesis; (a) Magnification: ×80000, (b) magnification: ×30000.

3.2.2 Characterization of inner-functionalized silica nanotube

FT-IR spectroscopy was firstly used to identify various functional groups inside the wall of silica nanotube after hydrophilic silane introduction (Figure 8). Pristine silica nanotube (blue line) displayed two strong peaks at 1080 cm^{-1} and 3400 cm^{-1}, which correspond to Si-O-Si stretching and hydroxyl group vibration, respectively. After VTMS silane treatment, the peak attributed to $C=CH_2$ vibration appeared at 3060 cm^{-1}. After APTES and CEST functionalization, 1° amine scissoring peak and C=O stretching peak 1635 cm^{-1} and 1715 cm^{-1} figured our respectively. Since the outer surface properties of silica nanotube cannot be altered due to contact of the nanotube with wall of AAO membrane, it is obvious that the functional group introduced by silane coupling agents is spatially controlled and limited in the inner surface of nanotubes.

In the same way, polymerization of hydrophilic polymer inside the pristine silica nanotube was realized. Surface polymerization of PAA on inner wall of silica nanotube was clarified by TEM and FT-IR analysis as shown in Figure 9 and 10. Average wall thickness of PAA-silica was measured to be ca. 50 nm (Figure 9b), which is thicker by 30 nm than that of pristine silica nanotubes (Figure 9a). Considering the increase of the wall thickness, carboxylic acid functional groups in inner wall of nanotubes was successfully introduced (Figure 10). Additionally, thermo-gravimetric analysis (TGA) was performed to investigate the precise weight percentages of the PAA moiety in the PAA-silica (Figure 11). The weight loss of

PAA-silica nanotube was higher than that of pristine silica nanotube by about 14%, which means successful introduction of PAA in inner wall of nanotube again.

To verify that the further treatment is limited to the inside, zeta (ζ)-potential value of each nanotube was also measured after template removal as well. Because the zeta-potential value of colloidal particles is generally obtained from outer layer in electrical double layer on outer surface of colloidal particles, inner functionalization may have no influence on zeta-potential value. As shown in Table 1, zeta potential of pristine, vinyl and PAA-silica show similar value (about -45~49 mV). On the other hand, for comparison, when the harvested pristine silica nanotubes were treated with CEST after template removal (outer surface functionalization), much lower value (-63.23 mV) of zeta potential can be obtained. In addition, similar value of zeta potential in PAA-silica nanotubes means outer surface remains silica itself, and therefore implies possible additional functionalization.

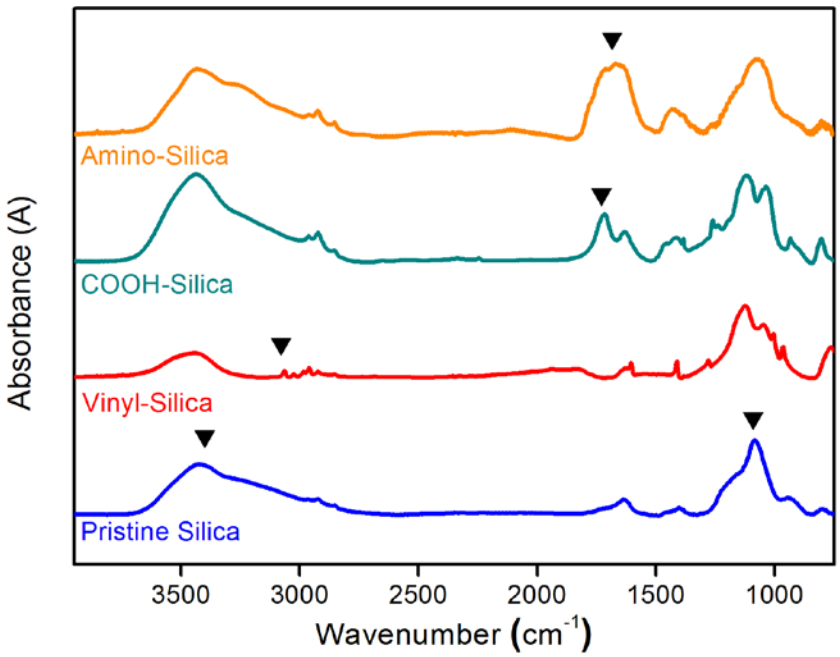

Figure 8. FT-IR spectra of 3 types of silane-treated silica nanotube. (Respective silane-treated silica nanotubes were denoted as; VTMS-treated silica nanotube: Vinyl-silica; CEST-treated silica nanotube: COOH-silica; APTES-treated silica nanotube: Amino-silica).

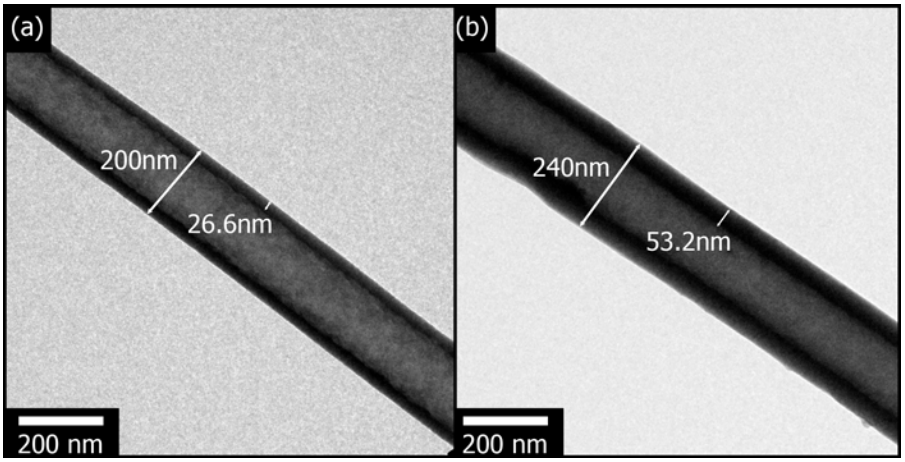

Figure 9. TEM images of a) pristine silica nanotube and b) PAA-silica nanotube

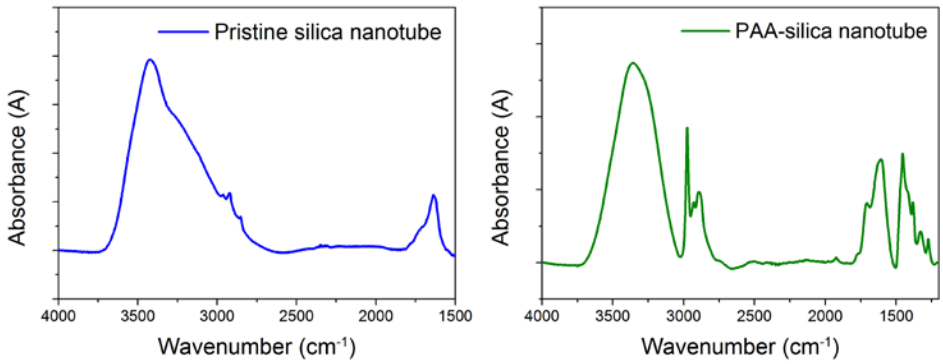

Figure 10. FT-IR spectra of pristine silica nanotube (blue) and PAA-silica nanotube (olive).

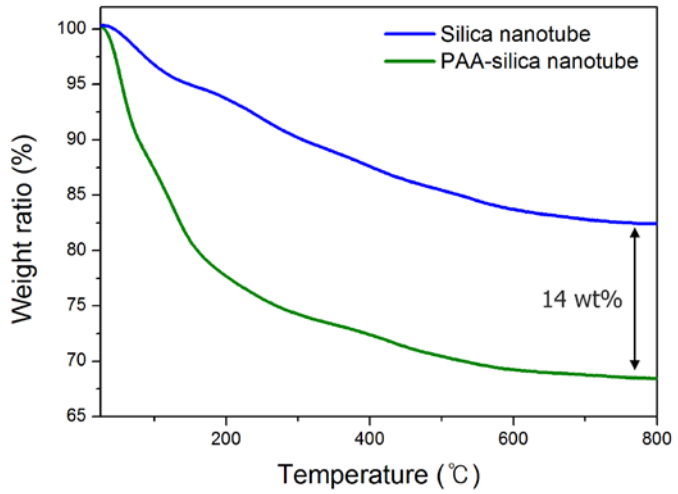

Figure 11. Thermogravimetric analysis (TGA) spectrum of pristine silica (blue line) and PAA-silica (olive line).

Table. 1. Zeta potential values of PAA- and silane- treated silica nanotube (Dispersed in water, all solutions adjusted to pH 7)

Entry	Material	Treatment	Zeta value
1	Pristine silica		-48.30 mV
2	Vinyl-Silica	VTMS (Vinyltrimethoxysilane)	-48.91 mV
3	PAA-silica	Poly (acrylic acid)	-44.27 mV
4	COOH-silica (Outside)	CEST (Carboxyethylsilane Triol)	-63.23 mV

3.2.3 SEM and EDX results of bifunctional silica nanotube

The bifunctional silica nanotube was prepared after successful introduction of PAA to the inner wall of pristine silica nanotube. The PAA-silica was obtained from AAO by hydrochloric acid etching and the PAA-silica powder was further treated with TTS in the reaction vessel. In the SEM mages of the PAA-silica after outer-wall treatment (Figure 12a), the bifunctional nanotubes exhibited almost same morphology with pristine silica nanotube. However, after TTS treatment on the outer surface, the surface of F-PAA-silica was slightly coated with the fluorine-containing silane with glittering surface. Following EDX analysis result, the surface of F-PAA-silica (Figure 12b) showed that fluorine element emerged due to TTS treatment, while carbon and oxygen element were attributed to both TTS and PAA layer in F-PAA-silica. Further FT-IR measurement on F-PAA-silica (Figure 13) exhibited peaks credited to CF_3CF_2-group at 1350-1320 cm^{-1}, with peaks related to the strong coupling of C-F and C-C stretching at 1240-1120 cm^{-1}, correspondingly. The result indicates that introduction of fluorine-functional group on outer wall of silica nanotube can be realized in the presence of polymer layer inside.

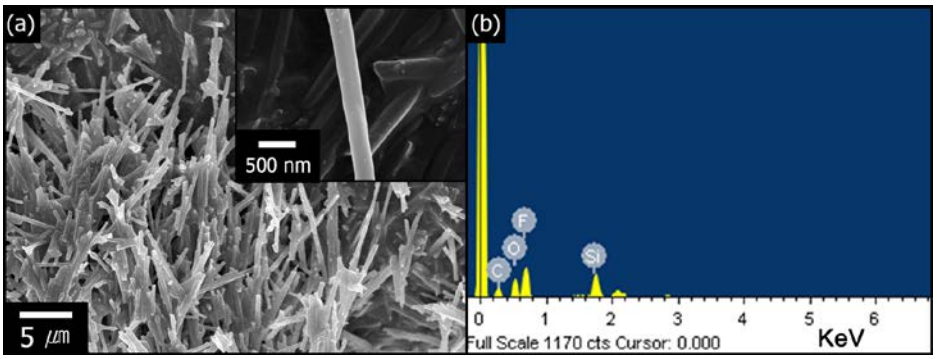

Figure 12. a) SEM image of TTS-treated PAA-silica (F-PAA-silica) (Inset: magnified SEM image on TTS-treated PAA-silica); b) EDX analysis spectrum of F-PAA-silica.

(a)

Element	Atomic%	Weight%
Carbon	33.43	23.94
Oxygen	21.53	20.54
Fluorine	36.75	41.64
Silicon	8.28	13.87

(b)

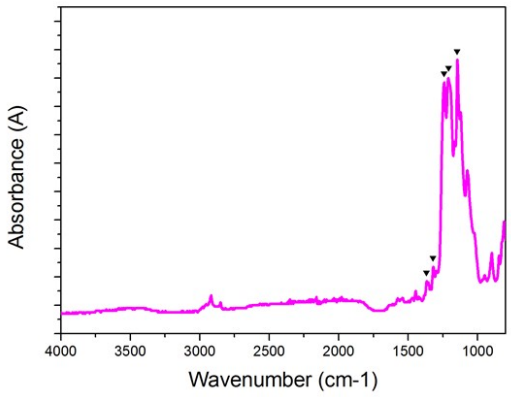

Figure 13. a) Table of elemental ratio for TTS-treated PAA-silica (F-PAA-silica); b) FT-IR spectrum of F-PAA-silica nanotube

3.3 Heck reaction of the Pd-inserted bifunctional silica nanotube (Pd-F-PAA-silica)

Figure 14 illustrates the brief procedure of introduction of palladium (Pd) nanoparticle inside the bifunctional silica nanotube. The degree of Pd nanoparticle insertion was optimized by 2.5×10^{-3} M as much as possible at a level that does not interfere the nanochannels varying the concentration of palladium chloride from 1×10^{-3} M to 5×10^{-3} M as shown in Figure 15 [62].

Table 2 demonstrates the catalytic activity of Pd-inserted silica nanotubes for three types of olefination of aryl iodides. In case of aryl iodide for Heck reaction, the condition of ligand group for palladium is much milder than other ligand group for the reaction [55-56] and the absence of ligand group makes overall reaction simple. For this reason, simple and widely used 3 types of aryl iodides [55] were chosen. In our work, n-Butyl acrylate was reacted with 4-iodoanisole (Entry 1), 2-iodotoluene (Entry 2) and styrene was reacted with iodobenzene (Entry 3).

The reaction was conducted at N,N-dimethylacetamide (DMA) containing tributylamine for recycling the Pd catalyst at reduction elimination step [54] and Pd inserted bifunctional silica nanotube in nitrogen atmosphere. In the result of Heck reaction, trans (*E*) type alkene product was synthesized by removing the iodide ion.

When the reaction was over, the product solution was filtered and conversion yield was clarified by gas chromatography/mass spectrometry (GC/MS). The reaction yield

was obtained by calculating the proportional amount of the reactants changed before and after the reaction comparing the reference material (pyrene, anthracene). The calculated yield was 99%, 99% and 98% for olefination of 4-iodoanisole (Entry 1), 2-iodotoluene (Entry 2) and iodobenzene (Entry 3), respectively. This outstanding performance is due to successful introduction of nano-sized Pd particle inside the bifunctional silica nanotube and open-type structure silica nanotube.

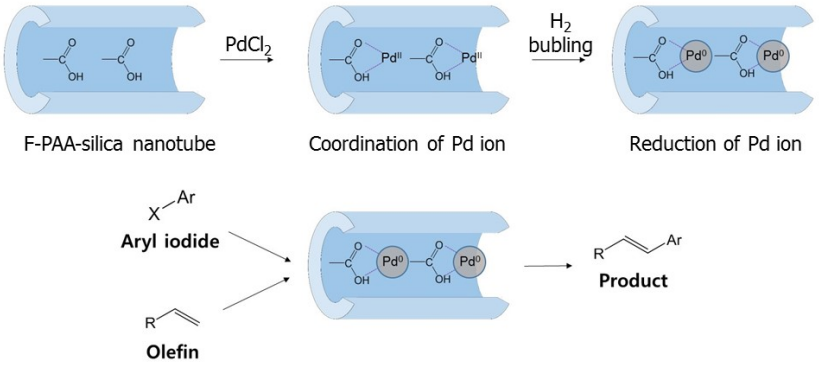

Figure 14 Schematic illustration of the insertion process of palladium inside the bifunctional silica nanotube and the Heck reaction process

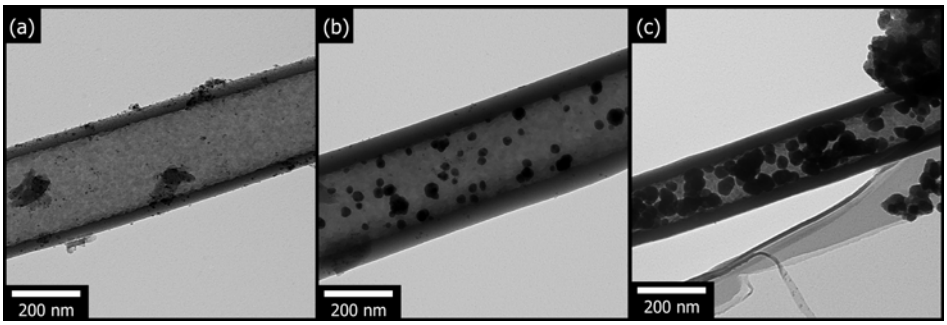

Figure 15. TEM image of Pd-F-PAA-silica nanotubes produced by varying concentration of $PdCl_2$; $PdCl_2$ concentration of (a) 1.0×10^{-3}M, (b) 2.5×10^{-3}M and (c) 5.0×10^{-3}M.

Table 2. The efficiency of olefination of aryl iodides. The yield was calculated by comparing corresponding GC-MS peak before and after reaction.

Entry	Aryl iodide	Olefin	t[h]	Product	Yield[%]
1			4		99 %
2			4	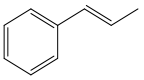	99 %
3		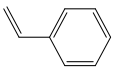	4	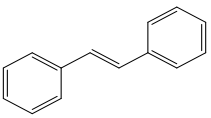	98 %

Chapter 4. Conclusion

In conclusion, silica nanotube with *ca.* 200nm diameter was fabricated by vapour phase synthesis using AAO membrane as hard template. Inner wall of silica nanotube was functionalized with acrylic acid by vapor deposition polymerization and investigated by SEM, TEM and FT-IR. The PAA coated silica nanotube was further functionalized with TTS, forming asymmetrically functionalized silica nanotube. The properties altered by functionalization was identified by zeta potential, EDX, TGA and FT-IR. Bifunctional silica nanotube was further treated with palladium chloride solution to introduce palladium salt inside the silica nanotube and the population of deposited palladium salt was optimized by adjusting $PdCl_2$ concentration. The nano-sized Palladium salt was reduced by bubbling hydrogen gas and resulting palladium nanoparticle was put into the inner surface of the functionalized silica nanotube successfully. The introduction of palladium was verified by TEM. The silica nanotube containing palladium was used as catalyst nanocarrier for Heck reaction of olefination and the highest efficiency 99% was identified by GC-MS. The fabrication of bifunctional silica nanotube and selective insertion of palladium may be expanded to selective insertion of metal nanoparticle and application for nanocatalyst in hydrophobic media.

References

[1] H. Peng, L. Zhang, C. Soeller, J. Travas-Sejdic, *Biomaterials*, **2009**, *30*, 2132.

[2] H. Yoon, J. Jang, *Adv Func. Mater*, **2009**, *19*, 1567.

[3] A. Nel, T. Xia, L. Madler N. Li, *Science*, **2006**, *311*, 622.

[4] L. Pan, M. Gu, G. Ouyang, C.Q. Sun, *Key Eng. Mater*, **2010**, 444, 17.

[5] C. R. Kothapalli, M. T. Shaw, M. Wei, *Acta Biomaterialia*, **2005**, 1(6), 653.

[6] J. Jang, *Adv. Polym. Sci*. **2006**, *199*, 189.

[7] A. -H. Lu, W. Schmidt, N. Matoussevitch, H. B. Knnemann, B. Spliethoff, B. Tesche, E. Bill,W. Kiefer, F. SchLth, *Angew. Chem*. **2004**, 116, 4403; *Angew. Chem. Int. Ed*. **2004**, 43, 4303.

[8] S. C. Tsang, V. Caps, I. Paraskevas, D. Chadwick, D. Thompsett, *Angew. Chem*. **2004**, 116, 5763; *Angew. Chem. Int. Ed*. **2004**, 43, 5645.

[9] Y. Jiang, Q. Gao, *J. Am. Chem. Soc*. **2006**, 128, 716.

[10] B. Yoon, C. M. Wai, *J. Am. Chem. Soc*. **2005**, 127, 17174.

[11] G. Korneva, H. Ye, Y. Gogotsi, D. Halverson, G. Friedman, J. -C. Bradley, K. G. Kornev, *Nano Lett*, **2005**, 5, 879.

[12] A. Perro, S. Reculusa, S. Ravaine, E. Bourgeat-Lami, E. Duguet, *J. Mater. Chem*, **2005**, 15, 3745.

[13] A. Walther, A.H.E. Müller, *Soft Matter*, **2008**, 4, 663.

[14] F. Wurm, A.F. Kilbinger, *Angew. Chem. Int. Ed*, **2009**, 48, 8412.

[15] S. Jiang, Q. Chen, M. Tripathy, E. Luijten, K. S. Schweizer, S. Granick, *Adv. Mater*, **2010**, 22, 1060.

[16] D. Dendukuri, P. S. Doyle, *Adv. Mater*, **2009**, 21, 4071.

[17] K. J. Lee, J. Yoon, J. Lahann, Curr. Opin. *Colloid Interface Sci*, **2011**, 16, 195.

[18] J. Yoon, K. J. Lee, J. Lahann, *J. Mater. Chem*, 2011, 21, 8502.

[19] S. C. Glotzer, M. J. Solomon, *Nature Materials*, **2007**, 6, 557

[20] C. H. Choi, D. A. Weitz, C. S. Lee, *Adv. Mater*, **2013**, 25, 2536.

[21] O. Gunduz, Z. Ahmad, E. Stride, M. Edirisinghe, *Mater. Sci. Eng. C Mater*, **2012**, 32, 1005.

[22] P. M. Valencia, O. C. Farokhzad, R. Karnik, R. Langer, *Nature Nanotechnology*, **2012**, 7, 623.

[23] D . Dendukuri, S. S. Gu, D. C. Pregibon, T. A. Hatton, P. S. Doyle, *Lab Chip*, **2007**, 7, 818.

[24] J. Lee, P. W. Bisso, R. L. Srinivas, J. J. Kim, A. J. Swiston, P. S. Doyle, *Nat. Mater*, **2014**, 13, 524.

[25] W. E. Uspal, H. Burak Eral, P. S. Doyle, *Nat. Commun*, 4, 2666.

[26] J. Lahann, *Small*, **2011**, 7, 1149.

[27] S. Rahmani, J. Lahann, *MRS Bulletin*, **2014**, 39, 251.

[28] W. O. Yah, A. Takahara, Y. M. Lvov, *J. Am. Chem. Soc*, **2012**, 134 (3), 1853.

[29] M. Ben-Ishai, F. Patolsky, *J. Am. Chem. Soc*, **2011**, 133 (5), 1545.

[30] Y. Xia, P. Yang, Y. Sun, Y. Wu, B. Mayers, B. Gates, Y. Yin, F. Kim, H. Yan, *Adv. Mat*. **2003**, 15, 5, 353.

[31] J.Jang, *Adv Polym Sci*, **2006**, 199, 189.

[32] Zhang. C, Yan. Y, Sheng Zhao. Y, Yao. J, *Annu. Rep. Prog. Chem, Sect. C: Phys.*

Chem, **2013**, 109, 211.

[33] A. L. Briseno, S. C. B. Mannsfeld, S. A. Jenekhe, Z. Bao, Y. Xia, *Material Today*, **2008**, 11 , 4, 38.

[34] C. N. R. Rao, Achutharao Govindaraj, *Adv. Mater*. **2009**, 21, 4208.

[35] H. J. Fan, P. Werner, M. Zacharias, *Small*, **2006**, 2, 6, 700.

[36] Y. Xia, P. Yang, Y. Sun, Y. Wu, B. Mayers, B. Gates, Y. Yin, F. Kim, H. Yan, *Chem. Soc. Rev*, **2011**, 40, 2986-3004

[37] C. R. Martin, *Science*, **1994**, 266, 1961.

[38] R . Gangopadhyay, *Encyclo Nanosci Nanotech*, **2004**, 2,105

[39] C. R. Martin, *Acc Chem Res*, **1995**, 28,61.

[40] M. Wan, *Encyclo Nanosci Nanotech*, **2004**, 2,153.

[41] C. R. Martin, T.A. Skotheim, R. L. Elsenbaumer, J. R. Reynolds, *Handbook of Conducting Polymers*, **1998**, ch 16, 2nd ed. Marcel Dekker, New York

[42] G. Omerz-Kaifer, P. A. Reddy, C. D. Gutsche, L. Echegoyen, *J Am Chem Soc*, **1998**, 120, 2486.

[43] S. M. Marinakos, L. C. Brouseau, A. Jones, D. L. Feldheim, *Chem Mater*, **1998**, 10, 1214

[44] J. Jang, B. Lim, J. Lee, T. Hyeon, *Chem Commun*, **2001**, 83.

[45] B. H. Hong, J. T. Lee, C. W. Lee, J. C. Kim, S.C. Bae, K.S. Kim, *J Am Chem Soc*, **2001**, 12, 10748

[46] M. Delvaux, J. Duchet, P. Y. Stavaux, R. Legras, S. Demoustier-Champagne, *Synth Met*, **2000**, 113, 275

[47] J. H. Chen, Z. P. Huang, D. Z. Wang, S. X. Yang, W. Z. Li, J. G. Wen, Z. F. Ren, *Synth Met*, **2000**, 125, 289

[48] J. Jang, J.H. Oh, *Chem. Commun*, **2004**, 882-883

[49] K. J. Lee, S. H. Min, J. Jang, *Chem. Eur. J.* **2009**, 15, 2491.

[50] T. Mizoroki, K. Mori, A. Ozaki, Bull. Chem. Soc. Jpn. **1971**, *44*, 581.

[51] R. F. Heck, J. P. Nolley, J. Org. Chem. **1972**, *37(*14), 2320.

[52] R. F. Heck, *Palladium Reagents in Organic Synthesis*, Academic Press: London, **1985**.

[53] R. F. Heck, *Org. React*, **1982**, 27, 345.

[54] W. Cabri, I. Candiani, *Acc. Chem. Res*., **1995**, 28, 2.

[55] R. M. Moriarty, W. R. Epa, A. K. Awasthi, *J. Am. Chem. Soc.*, **1991**, 113 (16), 6315.

[56] W. Cabri, *Chim. Ind. (Milan)*, **1993**, 75, 314 and references therein.

[57] R. Kumar, A. Shard, R. Bharti, Y. Thopate, A. Kumar Sinha, *Angew Chem Int. Ed*, **2012**, 51, 2636.

[58] A. Yamaguchi, F. Uejo, T. Yoda, T. Uchida, Y. Tanamura, T. Yamashita, N. Teramae, *Nature Materials*, **2004**, 3, 337

[59] A. Yamaguchi, J. Watanabe, M. M. Mahmoud, R. Fujiwara, K. Morita, T. Yamashita, Y. Amino, Y. Chen, L. Radhakrishnan, N. Teramae, *Analytica Chimica Acta*, **2006**, 556, 157.

[60] J. C. Forsyth, W. E. Baker, K. E. Russell, R. A. Whitney, *Journal of Polymer Science Part A: Polymer Chemistry*, **1997**, 35, 16, 3517.

[61] J. Dziczkowski, V. Dudipala, M. D. Soucek, *Progress in Organic Coatings*, **2012**, 73, 308.

[62] S. Ko, J. Jang, *Angew. Chem. Int. Ed*. **2006**, 45, 7564.

초 록

다양한 기능을 가진 비등방성 물질의 제조는 최근 널리 연구되고 있는 분야이며, 또한 상기 물질을 마이크로/나노 크기로 제조하여 촉매 등으로 응용하는 것은 전형적인 벌크 물질에 비해 높은 효율을 보이기 때문에 이점이 있다. 안팎이 다른 작용기를 가진 비등방성 나노 물질은 선택적인 나노캐리어와 스마트 나노촉매로 활용될 수 있다. 이 논문에서는, 요오드화 아릴의 올레핀화 반응을 위해 실리카 나노튜브를 양극 산화 알루미늄(AAO)을 경형판으로 이용한 기상 합성법(VPS)으로 제조하였고 카복시기를 실리카 나노튜브 내부에 도입하였다. 그 후, 실리카 나노튜브 외벽에 추가적인 소수성 실란 처리를 통해 안팎 다른 성질의 두 가지 작용기를 가진 실리카 나노튜브를 선택적으로 제조하였다. 그 후, 팔라듐 이온을 나노튜브 내부에 삽입하고 수소 기체로 팔라듐 이온을 환원시켜 팔라듐 나노입자를 제조하였으며 위 나노입자는 실리카 나노튜브 내벽의 카복시기와 배위 결합할 수 있다. 3가지 종류의 요오드화 아릴의 올레핀화 반응이 팔라듐이 삽입된 실리카 나노튜브를 통해 이루어졌고, 최대 올레핀화 반응 효율은 99%였다. 이 논문에서와 같은 신규한 접근은 나노촉매 응용을 위한 비등방성 캐리어의 제조를 위한 새로운 방법을 창출할 것으로 사료된다.

주요어 : 실리카 나노튜브, 나노캐리어, 나노 촉매, VDP, Heck 반응, 비등방성 물질, 양극 산화 알루미늄(AAO)

학번 : 2013-23164